Cell Cycle Regulation of E2F Site Occupation in Vivo

Jörk Zwicker, Ningshu Liu, Kurt Engeland, Frances C. Lucibello, Rolf Müller*

DNA-binding E2F complexes have been identified throughout the mammalian cell cycle, including the transcriptionally inactive complexes with pocket proteins, which occur early in the prereplicative G_1 phase of the cycle, and the transactivating free E2F, which increases in late G_1. Here, a regulatory B-*myb* promoter site was shown to bind with high affinity to free E2F and to E2F–pocket protein complexes in an indistinguishable way in vitro. In contrast, in vivo footprinting with NIH 3T3 cells demonstrated E2F site occupation specifically in early G_1, when the B-*myb* promoter is inactive. These observations indicate that a novel mechanism governs E2F-DNA interactions during the cell cycle and emphasize the relevance of E2F site–directed transcriptional repression.

Despite the central role of E2F in cell cycle–regulated transcription and the identification of multiple DNA-binding E2F complexes in nuclear extracts in vitro (*1*, *2*), no data are available concerning the interaction of E2F complexes with target promoters in vivo. To address this question, we chose the B-*myb* gene (*3*) as a model. Transcription of the B-*myb* gene in mouse fibroblasts greatly increases in late G_1 and reaches a peak in the S phase of the cell cycle, when DNA replication takes place (*3*). Structure-function analysis of the B-*myb* promoter identified an element necessary for cell cycle regulation, CTTGGCGG, close to the transcription start sites (*3*). This element represents a potential E2F site, because protein binding in cell extracts is efficiently inhibited by the adenovirus E2A promoter E2F site. Mutation of this site leads to up-regulation of transcription in G_0 cells, which implies that the interacting protein complex acts as a repressor. In vitro experiments with cell extracts suggested that the G_0 complex contains the p107 pocket protein (*4*). In contrast, free E2F is found in cell extracts throughout the cell cycle, and other higher order DNA-binding complexes are detected around S-phase entry (*4*). The function of these complexes remains elusive, although the formation of free E2F is generally believed to play a role in E2F site–dependent gene activation (*1*).

To analyze the interaction of the putative B-*myb* E2F site with E2F complexes in a more direct way, we reconstituted in vitro different dimeric and trimeric E2F complexes from recombinant proteins and studied their interaction with the B-*myb* E2F site by means of electrophoretic mobility-shift assay (EMSA) (*5*) and methylation protection footprinting (*6*). The complexes E2F-1–DP-1, E2F-1–DP-1–pRb (*2*, *7*), E2F-4–DP-1, and E2F-4–DP-1–p107 (*8*) bound to the B-*myb* E2F site with comparable efficiency, and with an affinity similar to that with which they bound to the high-affinity adenoviral E2A promoter site (*9*), as determined by quantitation of the data (*10*) (Fig. 1A). Very similar results were obtained with complexes containing E2F-2, E2F-3, E2F-5, DP-2, and DP-3 (*11*). As expected, binding was abolished when a point mutation was introduced into the E2F site (CTTGGCGG → CTTGGCTG) (*10*).

The E2F-4 complexes were chosen for in vitro dimethyl sulfate (DMS) protection footprinting analysis (*6*) because p107 is a major pocket protein component in E2F complexes that interact with the B-*myb* E2F site in nuclear extracts (*4*) and because E2F-4 is the only known E2F family member that interacts with p107 (*8*). Six guanine residues were protected in the region of the E2F site [*CTTGGCGGGAG* (E2F site in italics, protected guanines underlined)]; the two most 3′ guanine residues downstream of the E2F site core motif showed partial protection (Fig. 2). No differences were detectable among the in vitro footprints obtained with E2F-4–DP-1 (free E2F) and E2F-4–DP-1–p107, respectively. Thus, E2F complexes, regardless of the presence of a pocket component, can be detected by methylation protection footprinting and show indistinguishable base contacts in vitro.

We next analyzed whether the E2F-4–DP-1 and E2F-4–DP-1–p107 complexes might display different affinities for the B-*myb* E2F site by determining the respective association and dissociation rates (on- and off-rates) (*12*). Again, the differences between the two complexes were either insignificant (on-rates) or indicated a slightly higher affinity of free E2F (off-rates) (Fig. 1B). This finding indicates that the p107 pocket protein component does not influence the DNA-binding affinity of E2F-4–DP-1 to any major extent—and in particular, not in a way that could explain the results obtained by in vivo footprinting described below. In addition, on- and off-rates were determined for E2F complexes identified in nuclear extracts and were found to be very similar (*13*), thus supporting the validity of the observations made with the recombinant proteins.

To analyze the role of the E2F site in vivo in further detail, we performed genomic DMS footprinting (*14*–*16*). NIH 3T3 cells synchronized in G_0 by serum deprivation and stimulated with 10% fetal bovine serum (FBS) were analyzed for cell cycle progression (DNA content), B-*myb* mRNA expression, and E2F site occupation (methylation protection) in vivo at various time points after stimulation. Serum stimulation of the quiescent cells led to S-phase entry

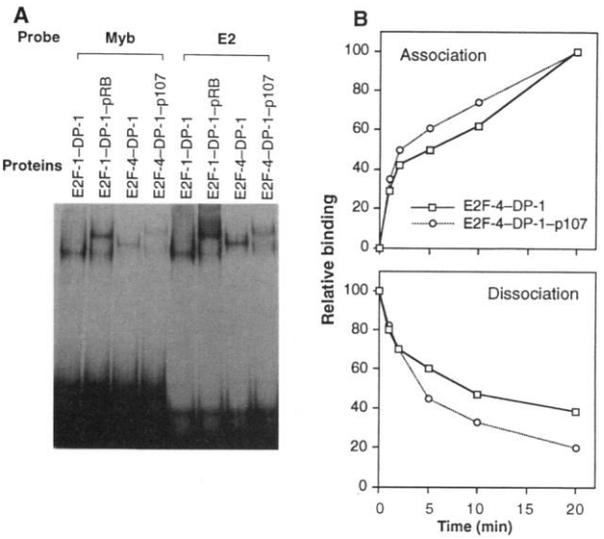

Fig. 1. (**A**) Interaction of the B-*myb* E2F site with different E2F–DP-1 and E2F–DP-1–p107 complexes in vitro. Complexes were reconstituted from recombinant GST fusion proteins and analyzed by EMSA (*5*, *10*) with the use of a synthetic oligonucleotide harboring either the B-*myb* E2F site (*3*) or an E2A promoter E2F site (*9*). The differences in intensity between the E2F-1 and E2F-4 complexes reflect variations in the E2F protein preparations rather than different binding affinities. (**B**) On- and off-rates of E2F-DNA complexes. E2F-4–DP-1 and E2F-4–DP-1–p107 complexes were analyzed by EMSA as described (*12*).

Institut für Molekularbiologie und Tumorforschung, Philipps-Universität Marburg, Emil-Mannkopff-Strasse 2, D-35033 Marburg, Germany.

*To whom correspondence should be addressed.

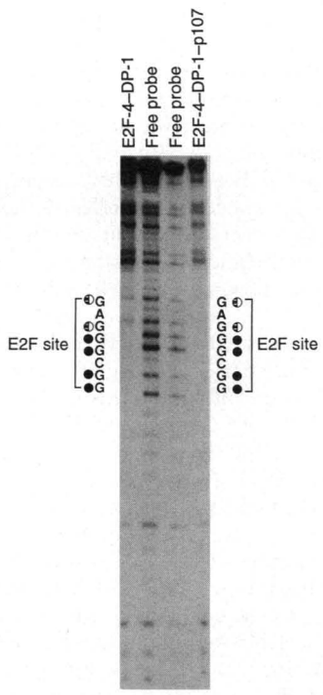

Fig. 2. In vitro methylation protection footprints of E2F-4–DP-1 and E2F-4–DP-1–p107 complexes. Methylated complexes were separated by EMSA (see Fig. 1A) and analyzed for protected guanine residues (*6*). ●, Full protection; ◐, partial protection.

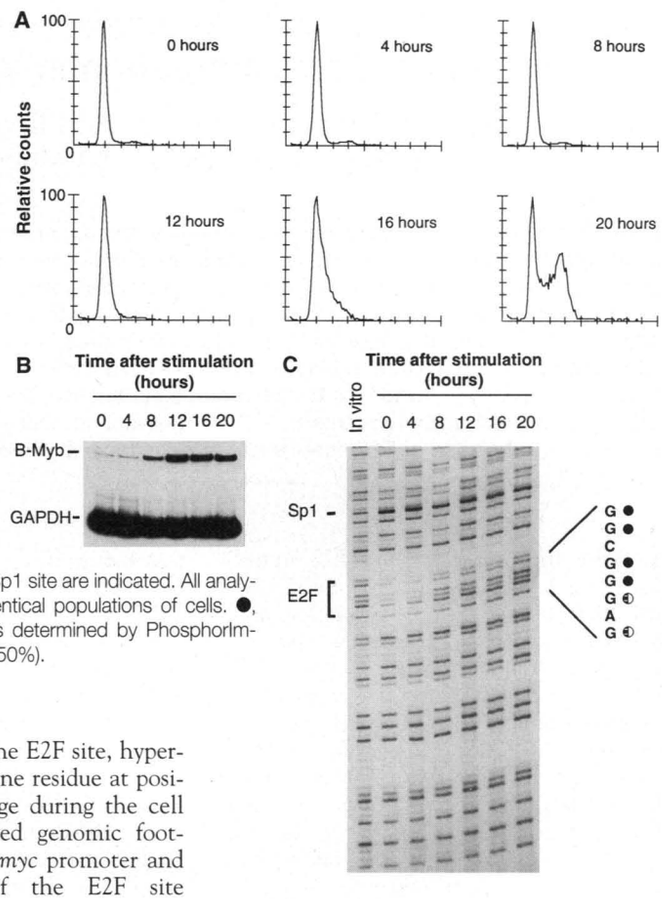

Fig. 3. Kinetics of B-*myb* mRNA expression and E2F site occupation in vivo. (**A**) Cell cycle analysis of NIH 3T3 cells synchronized in G_0 by serum deprivation and stimulated with 10% FBS. Cells were stained for DNA content with Hoechst 33258 and analyzed by fluorescence-activated cell sorting (*14*). (**B**) Expression of B-*myb* mRNA during the cell cycle, as measured by RT-PCR (*22*). Glyceraldehyde-3-phosphate dehydrogenase (GAPDH) was included as a control. (**C**) Genomic DMS footprinting (*14–16*) of the B-*myb* core promoter region (coding strand) at different stages of cell cycle progression. The E2F site and a potential Sp1 site are indicated. All analyses were performed with identical populations of cells. ●, Strong protection (>80%, as determined by PhosphorImager); ◐, partial protection (~50%).

after ~12 hours (Fig. 3A). As reported previously (*3*), B-*myb* mRNA expression increased 8 hours after stimulation (that is, in mid- to late G_1) and reached a peak at 12 hours, the time of S-phase entry (Fig. 3, A and B).

Analysis of G_0 cells by genomic footprinting (Fig. 3C) revealed a clear occupation of the E2F site core sequence and two guanine residues located immediately downstream. Thus, six guanine residues at positions –209, –208, –206, –205, –204, and –202 (relative to the ATG start codon) (*3*) were clearly protected; the latter two positions showed partial protection. This protection pattern is very similar to that seen in vitro (Fig. 2), which supports the conclusion that the protein complex interacting in vivo is indeed E2F. In addition, a guanine residue at position –223 was hypermethylated. This region of the B-*myb* promoter encompasses a potential Sp1 site. However, because Sp1 sites usually show protection rather than hypermethylation in vivo (*17*), the nature of the observed hypermethylation remains unclear. Analysis of serum-stimulated cells showed a similar E2F site protection at 4 hours, but protection was acutely diminished at 8 hours, and at later time points no protection was detectable. This loss of protection coincided precisely with the onset of B-*myb* transcription (Fig. 3B). In contrast to the cell cycle–regulated protection of the E2F site, hypermethylation of the guanine residue at position –223 did not change during the cell cycle. We also performed genomic footprinting of the mouse c-*myc* promoter and observed protection of the E2F site throughout the cell cycle (*18*). This observation clearly indicates that DNA binding of late G_1- and S-phase E2F complexes is detectable by genomic footprinting, and thus strongly supports the validity of the results obtained with B-*myb*.

These results clearly suggest that the DNA-binding properties of the E2F complexes identified in late G_1-S extracts in vitro (free E2F and higher order E2F complexes) (*3*, *4*, *19*) are modulated by an unknown mechanism in vivo. It is possible that such a regulation involves the phosphorylation of E2F by certain cyclin-dependent kinases, as has been described for a cyclin A–associated kinase (*20*). Cyclin A, however, is unlikely to be responsible for the effects observed in our study, because it becomes active much later in the cell cycle, during S phase. It is also conceivable that a cell cycle–dependent alteration in the nucleoprotein structure of the B-*myb* promoter modulates the occupation of the E2F site, perhaps as a consequence of phosphorylation of the E2F pocket protein component or the establishment of higher order cyclin–cyclin-dependent kinase complexes.

Our findings also support the conclusion that E2F site–mediated transcriptional activation does not seem to play a crucial role, if any, in B-*myb* regulation, because the E2F site is unoccupied at a time when transcription increases. The principal mechanism of B-*myb* regulation during the cell cycle therefore appears to be transcriptional repression. This conclusion is in agreement with the mutational analysis of the B-*myb* promoter (*3*). This interpretation of the data would also be compatible with recent observations showing that pRb represses transcription through a mechanism that involves its tethering to the promoter through DNA-bound E2F (*21*). E2F site–dependent activation of B-*myb* may therefore be restricted to certain nonphysiological conditions such as viral infection, transformation, or E2F overexpression, during which it may provide an additional level of regulation.

REFERENCES AND NOTES

1. For reviews see K. Helin and E. Harlow, *Trends Cell Biol.* **3**, 43 (1993); N. B. La Thangue, *Curr. Opin. Cell Biol.* **6**, 443 (1994); R. Müller, *Trends Genet.* **11**, 173 (1995); J. R. Nevins, *Science* **258**, 424 (1992).
2. L. R. Bandara, J. P. Adamczewski, T. Hunt, N. B. La Thangue, *Nature* **352**, 249 (1991); S. P. Chellappan, S. Hiebert, M. Mudryj, J. M. Horowitz, J. R. Nevins, *Cell* **65**, 1053 (1991); T. Chittenden, D. M. Livingston, W. G. Kaelin, *ibid.*, p. 1073.
3. E. W.-F. Lam and R. J. Watson, *EMBO J.* **12**, 2705 (1993).
4. E. W.-F. Lam *et al.*, *ibid.* **13**, 871 (1994).
5. Glutathione-S-transferase (GST) fusion proteins were expressed in *Escherichia coli* and purified by affinity chromatography: E2F1, amino acids 87 to 1398 (*7*); E2F-4, full-length protein (*8*); pRb, amino acids 300 to 928 [R. Bernards *et al.*, *Proc. Natl. Acad. Sci. U.S.A.* **86**, 6474 (1989)]; and p107, amino

acids 744 to 2460 [M. E. Ewen, Y. Xing, J. B. Lawrence, D. M. Livingston, *Cell* **66**, 1155 (1991)]. For EMSAs [A. Barberis, G. Superti-Furga, M. Busslinger, *ibid.* **50**, 347 (1987)], the purified recombinant proteins (~100 ng) were incubated with 0.5 pmol of ^{32}P-labeled probe for 30 min at 22°C in 15 μl of a buffer containing 50 mM tris-HCl (pH 8.0), 50 mM NaCl, 10% (v/v) glycerol, 0.2 mM EDTA, 1 mM dithiothreitol, and polydeoxyadenylic-deoxythymidylic acid (poly[dA/dT]) (67 ng/μl). Probes were labeled by filling in 5′ overhanging ends of four to seven bases. Samples were run on 4% nondenaturing polyacrylamide gels in 0.5× tris-borate EDTA (TBE) at 4°C and 10 V/cm. Gels were exposed to x-ray films and quantitatively evaluated with a Molecular Dynamics PhosporImager. The following double-stranded probes were used: B-*myb* (*3*), 5′-GGCGCCGACGCACTTGGCGGGAGATAGGAAAGTGGTTCTGTG (E2F site underlined); mutated B-*myb* site, 5′-GGCGCCGACGCACTTGGCTGGAGATAGGAAAGTGGTTCTGTG; E2 promoter, 5′-gatcGACTAGTTTCGCGCCCTTTCTActag (lowercase letters represent unrelated sequences used for the fill-in labeling reactions); unrelated probe, 5′-GATCCTCTCACCTGCTGCTAG [NIP-5′; K. Engeland, N. C. Andrews, B. Mathey-Prevot, *J. Biol. Chem.* **270**, 24572 (1995)].
6. For in vitro DMS footprinting, a B-*myb* coding strand oligonucleotide was end-labeled, purified, and annealed to the noncoding strand. Binding reactions were carried out as described (*5*). Two microliters of 2% DMS were added, and the methylation reaction was stopped after 3 min by adding 2 μl of 60 mM β-mercaptoethanol. The samples were run on a 4% gel and transferred to ion-exchange paper. Both the shifted and unshifted (free probe) bands were cut out, rinsed with tris-EDTA (TE) buffer, and eluted with TE buffer containing 1.5 M NaCl at 65°C. The eluted DNA was extracted with chloroform, precipitated, and dissolved in water. Equal radioactive amounts of free probe and shifted complex were cleaved with 10% piperidine at 95°C for 30 min. The DNA was precipitated and loaded on a 15% denaturing acrylamide gel.
7. K. Helin *et al.*, *Cell* **70**, 337 (1992); W. G. Kaelin *et al.*, *ibid.*, p. 351.
8. R. L. Beijersbergen *et al.*, *Genes Dev.* **8**, 2680 (1994); D. Ginsberg *et al.*, *ibid.*, p. 2665.
9. M. Mudryj, S. W. Hiebert, J. R. Nevins, *EMBO J.* **9**, 2179 (1990).
10. EMSA gels were evaluated with a PhosphorImager to calculate the fraction of bound probe. The following fractions were obtained: E2 promoter E2F site, 1.0% (E2F1–DP-1) and 0.8% (E2F-4–DP-1), respectively; B-*myb*, 0.7% (E2F1–DP-1) and 2.0% (E2F-4–DP-1), respectively; mutated B-*myb*, <0.01%; unrelated probe, <0.002%.
11. K. Engeland and N. Liu, unpublished data.
12. On-rates and off-rates were determined essentially as described [R. Janknecht, R. A. Hipskind, T. Houthaeve, A. Nordheim, H. G. Stunnenberg, *EMBO J.* **11**, 1045 (1992)]. The data were quantitated with a PhosphorImager. For on-rates, recombinant protein complexes were incubated at 4°C with the B-*myb* probe (*5*) and, after different incubation times, loaded on a 4% gel run at 4°C. The latest time point was used for normalization of the results (100% value). For off-rates, recombinant protein complexes and radioactive DNA probe were incubated at 22°C for 20 min to achieve maximum binding. The samples were cooled to 4°C, and a 50-fold excess of nonradioactive competitor was added. After different incubation times, samples were analyzed by EMSA. A sample without competitor served as the reference for normalization (100% value).
13. N. Liu, unpublished data.
14. F. C. Lucibello *et al.*, *EMBO J.* **14**, 132 (1995).
15. G. P. Pfeifer, S. D. Steigerwald, P. R. Mueller, B. Wold, A. D. Riggs, *Science* **246**, 810 (1989).
16. Genomic DMS footprinting was performed as described (*14, 15, 17*). The following primers were used: primer 1, 5′-TCAGGACTCAGGCTGCT; primer 2, 5′-CGAGCCGCTCCGGGCCCCAGG; and primer 3, 5′-GGCCCCAGGCGGTGCTCTCAGGCG.
17. J. Zwicker *et al.*, *EMBO J.* **14**, 4514 (1995); J. Zwicker *et al.*, *Nucleic Acids Res.* **23**, 3822 (1995).
18. J. Zwicker, unpublished data. The c-*myc* E2F site is described in F. Oswald, H. Lovec, T. Möröy, M. Lipp, *Oncogene* **9**, 2029 (1994) and in the reviews in (*1*).
19. The formation of G_0-G_1 phase– and S phase–specific E2F complexes binding to the B-*myb* probe was confirmed in our own experiments with the use of extracts from NIH 3T3 cells (N. Liu, unpublished data).
20. W. Krek *et al.*, *Cell* **78**, 161 (1994); B. D. Dynlacht, O. Flores, J. A. Lees, E. Harlow, *Genes Dev.* **8**, 1772 (1994).
21. S. J. Weintraub *et al.*, *Nature* **375**, 812 (1995).
22. Isolation of RNA and reverse transcription polymerase chain reaction (RT-PCR) were performed exactly as described (*14, 17*). A region of B-*myb* complementary DNA (cDNA) from positions +1630 to +2228 was amplified with the use of the primers 5′-GACACCCCTGCACCAGAAGTATC and 5′-GGCTGGACTTCAGGCGGCT.
23. We thank W. Kaelin, R. Bernards, N. La Thangue, R. Weinberg, and D. Livingston for E2F, DP, pRb, and p107 cDNAs. Supported by grants from DFG and BMBF. J.Z. was the recipient of a fellowship from the Boehringer-Ingelheim Fonds.

20 September 1995; accepted 16 January 1996

Rapid Degradation of the G_1 Cyclin Cln2 Induced by CDK-Dependent Phosphorylation

Stefan Lanker, M. Henar Valdivieso, Curt Wittenberg*

Cyclins regulate the major cell cycle transitions in eukaryotes through association with cyclin-dependent protein kinases (CDKs). In yeast, G_1 cyclins are essential, rate-limiting activators of cell cycle initiation. G_1-specific accumulation of one G_1 cyclin, Cln2, results from periodic gene expression coupled with rapid protein turnover. Site-directed mutagenesis of *CLN2* revealed that its phosphorylation provides a signal that promotes rapid degradation. Cln2 phosphorylation is dependent on the Cdc28 protein kinase, the CDK that it activates. These findings suggest that Cln2 is rendered self-limiting by virtue of its ability to activate its cognate CDK subunit.

The term "cyclin" was originally coined to describe dramatic fluctuations in abundance displayed by the positive regulatory subunits of CDKs during the cell division cycle (*1*). Despite the fact that most cyclins accumulate periodically, the mechanisms governing their accumulation appear to differ. The budding yeast G_1 cyclins, encoded by the *CLN1* and *CLN2* genes, accumulate during the G_1 phase and become maximal during the late G_1 phase as cells transit the start (the point at which cells commit to completion of a new cell cycle). Because the Cln proteins appear to be constitutively unstable (*2–5*), their pattern of accumulation largely reflects their pattern of gene expression. G_1 cyclin abundance is important in determining the timing of cell cycle initiation. Consequently, Cln protein instability is critical for proper regulation of cell cycle progression.

The PEST sequence (Pro, Glu, Ser, and Thr), found in all three yeast G_1 cyclins, was originally identified as a potential determinant of protein instability on the basis of the frequency of its occurrence in constitutively unstable proteins (*6*). However, it has yet to be functionally defined. Deletion of the COOH-terminal sequences of Cln2 and Cln3 that include the PEST motif results in phenotypes consistent with hyperactivation of G_1 cyclins (*7*). Furthermore, these truncations, as well as more precise deletions of PEST sequences, partially stabilize the mutant proteins (*4, 5, 8*). However, it is not clear whether the PEST sequences per se or other aspects of the PEST-containing region constitute the relevant determinants. Our analysis of the posttranslational modification of Cln2 has demonstrated the importance of Cln2 phosphorylation as a signal for its rapid turnover. Because Cln2 phosphorylation is dependent on the activity of its cognate CDK subunit, we propose that phosphorylation of Cln2 by Cdc28 couples activation of the Cln2-Cdc28 protein kinase to degradation of the Cln2 polypeptide and, thereby, renders Cln2-activated CDK activity self-limiting.

Phosphorylation of Cln2 causes its heterogeneous electrophoretic mobility as observed by SDS–polyacrylamide gel electrophoresis (SDS-PAGE) (Fig. 1A). The Cln2 species with highest mobility comigrates with bacterially expressed Cln2 polypeptide (*2*). Treatment of ^{35}S-labeled Cln2 immunoprecipitates with calf intestine alkaline phosphatase in the absence, but not in the presence, of phosphatase inhibitors resulted in the loss of the species with lower mobility. In addition, Cln2 became isotopically labeled when cells were grown in the presence of [^{32}P]orthophosphate (Fig. 1B). The phosphorylated amino acid residues were primarily phosphoserine and, to a lesser extent, phosphothreonine (Fig. 1C) .

To identify the protein kinase responsi-

S. Lanker and C. Wittenberg, Departments of Molecular Biology and Cell Biology, Scripps Research Institute, La Jolla, CA 92037, USA.
M. H. Valdivieso, Edificio Departamental, Microbiologia, Biologia, Avenida Del Campo Charro s/n, 37007 Salamanca, Spain.

*To whom correspondence should be addressed.